Chinese Chemical Letters 36 (2025) 109778

Contents lists available at ScienceDirect

Chinese Chemical Letters

journal homepage: www.elsevier.com/locate/cclet

Rapid and specific fluorescent probe visualizes dynamic correlation of Cys and HClO in OGD/R

Pei Huang[a], Weijie Zhang[a], Junping Wang[a], Fangjun Huo[b,*], Caixia Yin[a,*]

[a] Institute of Molecular Science, Key Laboratory of Chemical Biology and Molecular Engineering of Ministry of Education, Shanxi University, Taiyuan 030006, China

[b] Research Institute of Applied Chemistry, Shanxi University, Taiyuan 030006, China

ARTICLE INFO

Article history:
Received 4 January 2024
Revised 12 March 2024
Accepted 14 March 2024
Available online 15 March 2024

Keywords:
Redox homeostasis
Dual-channel
OGD/R
Fluctuations
Peritonitis

ABSTRACT

Intracellular redox homeostasis is of indispensable importance in pathophysiology. In order to maintain the balance of the redox state within the cell, reactive oxygen species (ROS) and reactive sulfur species (RSS) react and transform with each other, and their levels also directly reflect the degree of oxidative stress and disease. Hypochlorous acid (HClO) and cysteine (Cys) usually co-exist in organisms, interacting with each other in many important physiological processes and synergistically maintaining the dynamic redox balance in the body. To understand the relevance and pathophysiological effects of these two signaling molecules in oxidative stress, unique fluorescence imaging tools are required. Herein, we designed and developed a dual-channel fluorescent probe **HP**, for the individual and continuous detection of HClO and Cys. This probe could simultaneously monitor the changes in the concentrations of HClO and Cys in cells, and was characterized by a fast response, high sensitivity and high selectivity, especially compared with glutathione (GSH) and homocysteine (Hcy), the probe had a good specificity for Cys. Importantly, probe **HP** successfully observed dynamic changes in HClO- and Cys-mediated redox status in the oxygen-glucose deprivation/reperfusion (OGD/R) model of HeLa cells and dynamically monitored fluctuations in endogenous HClO levels in lipopolysaccharides (LPS)-induced peritonitis mice.

Redox processes cover almost all the basic processes of life functions from bioenergetics to metabolism, so intracellular redox homeostasis is of great significance in the fields of physiology and pathology [1]. However, once the redox balance in the cell is disrupted, it can lead to a variety of physiological disorders and diseases, even tumor development [2–5]. Large or significant changes in the redox state can be buffered by redox-active molecules, which contribute to the dynamic equilibrium of the intracellular redox state through interactions and interconversions. Hypochlorous acid (HClO) is an important reactive oxygen species (ROS) that can be generated from hydrogen peroxide (H_2O_2) and chloride ions (Cl^-) and is closely related to the innate defences of the host and plays a crucial role in killing pathogens [6–8], however, its overproduction can lead to oxidative stress and cause inflammation. There is growing evidence of a strong link between HClO and a variety of biological and pathological activities ranging from inflammatory diseases to cancer, as well as immune and neurological disorders. Cysteine (Cys), one of the representatives of reactive sulphur (RSS), plays an important role in protein synthesis, gene regulation, free radical scavenging and anti-aging in animals [9–11]. Abnormal Cys concentrations in cells can be used as a biomarker for many diseases, such as cancer, inflammation, allergic skin damage, Alzheimer's disease and cardiovascular disease. Cys and HClO interact in many important physiological processes and are important mediators of brain function. *In vivo*, Cys acts as an antioxidant and inhibits HClO in oxidative stress, cytotoxicity, protein oxidation, and lipid peroxidation [12,13]. Therefore, the sequential or simultaneous detection of Cys and HClO contributes to the understanding of the interactions between these two substances in the cell and has a very important role in the assessment of their physiological and pathological processes.

Fluorescence imaging, characterised by non-invasive radiation, high sensitivity and spatial and temporal resolution, is a powerful tool for the visual and quantitative detection of biomolecules in biological systems [14–20]. Many sensitive and selective fluorescent probes have been developed for the detection of HClO or Cys [21–43]. However, these fluorescent probes do not meet the need for simultaneous detection of HClO, Cys and HClO/Cys. While it is possible to use two separate fluorescent probes for simultaneous detection of two analytes, the solution of simply mixing two

* Corresponding authors.
E-mail addresses: huofj@sxu.edu.cn (F. Huo), yincx@sxu.edu.cn (C. Yin).

https://doi.org/10.1016/j.cclet.2024.109778
1001-8417/

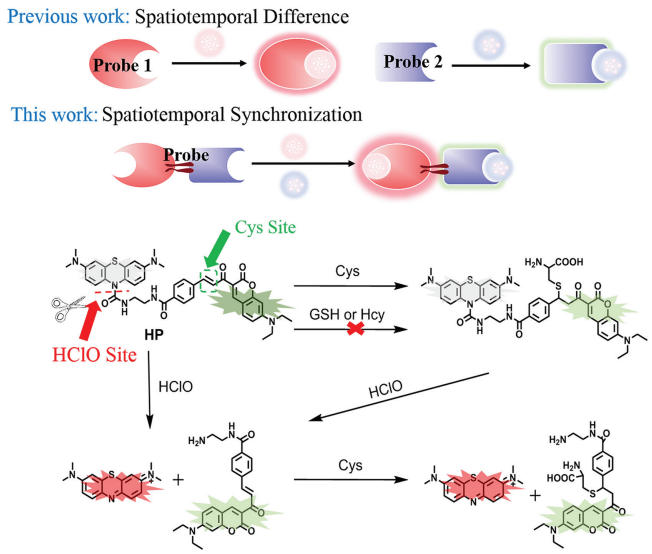

Scheme 1. Design strategy of the probe **HP**.

probes in a single system complicates the instrumental setup to achieve simultaneous sensing and potentially reduces the temporal resolution of fluorescence imaging. In addition, the two combined probes often have different chemical and biological properties *in vivo*, such as localisation and bleaching, and usually interfere with each other, thus impairing detection and sometimes even preventing quantitative analysis. Therefore, the development of dual response probes with independent signal units is an effective strategy to solve this problem.

Herein, we designed and synthesised a dual response fluorescent probe **HP** for the individual and sequential detection of Cys and HClO (Scheme 1). In the probe **HP**, ethylenediamine was used to link coumarin and methylene blue fluorescent reporter groups without fluorescence crosstalk, and α,β-unsaturated ketone bonds and amide bonds were the specific response sites for Cys and HClO, respectively. When the probe **HP** responded to Cys and HClO, due to the destruction of the conjugation and the breakage of the bond, the green fluorescence underwent a blue shift and the red fluorescence was triggered, achieving simultaneous and differentiated detection of Cys and HClO, with fast response and high sensitivity. Inspired by these salient features, probe **HP** was successfully applied to image exogenous and endogenous Cys and HClO in living cells, while the probe could monitor the fluctuation of HClO and Cys during oxygen-glucose deprivation/reperfusion (OGD/R). Moreover, probe **HP** was successfully used to monitor endogenous HClO level fluctuations in lipopolysaccharide (LPS)-induced peritonitis in mice. Therefore, we developed an effective tool to elucidate the redox dynamic balance of Cys and HClO in OGD/R, which had important guiding significance for the development of effective drugs for redox therapy-related diseases.

The probe **HP** was synthesized according to the synthesis steps in Supporting information. Firstly, we investigated the optical properties of the probe **HP** in the mixed system of PBS and CH_3CN (1/1, v/v, pH 7.4) in response to Cys and HClO respectively. As shown in Fig. 1, the probe **HP** showed an absorption band at 460 nm in the above system, and the gradual addition of HClO exhibited a new peak at 660 nm and a shoulder at 620 nm, with the new peak appearing as a characteristic absorption peak for methylene blue. Meanwhile, a significant increase in fluorescence emission intensity at 685 nm was attributed to the specific oxidation and breaking of the amide bond, which restored the red fluorescence of the methylene blue dye with an extensive π-conjugated structure, corresponding to the ultraviolet–visible (UV–vis) absorption spectral

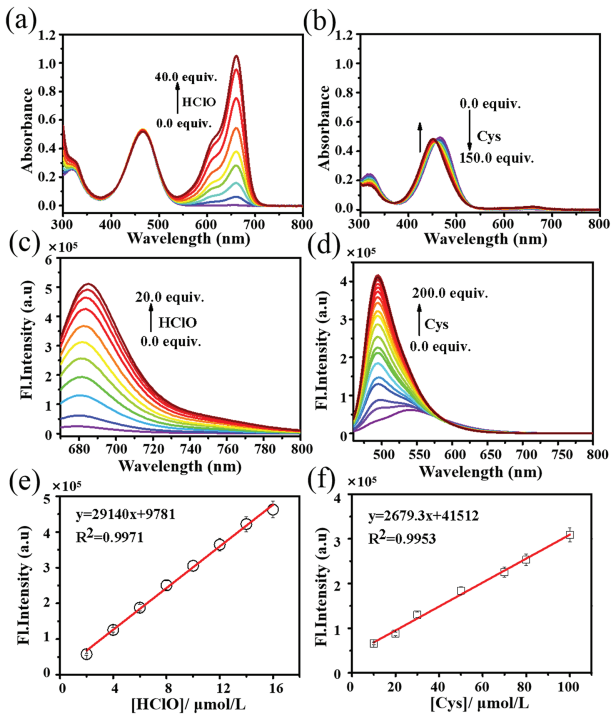

Fig. 1. Absorption spectral response (a) and fluorescence spectral response (c) of probe **HP** detecting HClO. (e) Linear relationship between fluorescence intensity and HClO concentration. Absorption spectral response (b) and fluorescence spectral response (d) of probe **HP** detecting Cys. (f) Linear relationship between fluorescence intensity and Cys concentration. Red channel: $\lambda_{ex} = 660$ nm, $\lambda_{em} = 685$ nm; green channel: $\lambda_{ex} = 450$ nm, $\lambda_{em} = 495$ nm.

results. Further, we evaluated the response of probe **HP** to Cys. The gradual addition of Cys resulted in a gradual weakening of the absorption band at 460 nm and the appearance of a new absorption band at 450 nm, which was attributed to the strong nucleophilicity of the sulfhydryl group in Cys, which underwent a nucleophilic addition with the α,β-unsaturated ketone in the probe **HP**, which then disrupted the conjugated structure of the probe and induced a blue shift. Moreover, the probe itself showed weak fluorescence emission at 550 nm, and the fluorescence intensity of the probe at 495 nm gradually increased with the gradual increase of Cys. The above results showed that the probe was able to achieve differential detection of HClO and Cys. In addition, the corresponding detection limits of the probe for HClO and Cys were 0.098 μmol/L and 0.079 μmol/L, respectively, according to the International Union of Pure and Applied Chemistry (IUPAC) definition (limit of detection (LOD) = $3S_b/m$). The results illustrated that the response patterns of the probe to HClO and Cys could be well differentiated in signals due to the introduction of different fluorescent molecules.

Subsequently, we evaluated the cascade response pattern of probe **HP** to HClO and Cys. As shown in Fig. 2, in the UV absorption spectrum, with the continuous addition of HClO, the maximum peak at 660 nm and the shoulder peak at 620 nm showed the characteristic absorption peaks of methylene blue, and when the peak tended to stabilise and then continued to add Cys, the absorption peak at 460 nm was gradually blue-shifted. Correspondingly, after the reaction of probe **HP** with HClO, the fluorescence of the probe peaked at 685 nm, and then with the continued addition of Cys, the fluorescence emission spectrum of the probe was blue-shifted, and the fluorescence at 495 nm was also gradually enhanced with the increase of Cys concentration. In contrast, only a decrease in the absorption peak at 460 nm, as well as a blue shift, was observed when the probe first responded to Cys. Interestingly, by gradually increasing HClO, the characteristic absorption

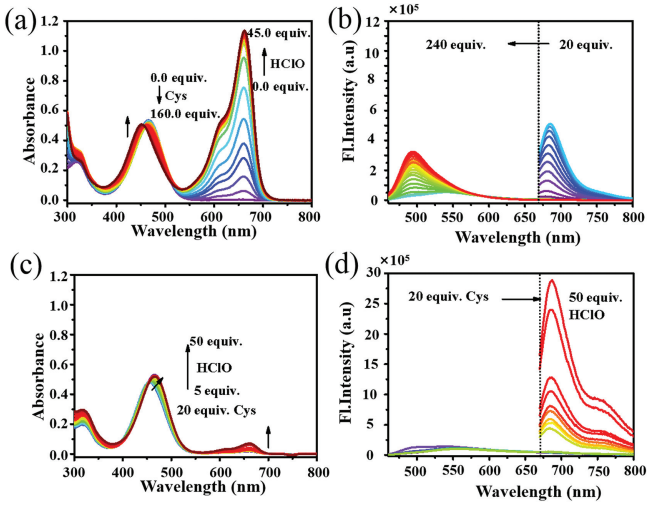

Fig. 2. (a) Changes of absorption spectra of probe **HP** (10 μmol/L) with the addition of first HClO (0–45.0 equiv.) and then Cys (0–160.0 equiv.). (b) Changes of the fluorescence spectrum of probe **HP** (10 μmol/L) with the addition of first HClO (0–20.0 equiv.) and then Cys (0–240.0 equiv.). Changes of absorption spectra (c) and fluorescence spectrum (d) of probe **HP** (10 μmol/L) with the addition of first 20.0 equiv. Cys and then HClO (5–50.0 equiv.). λ_{ex} = 660 nm and λ_{ex} = 450 nm.

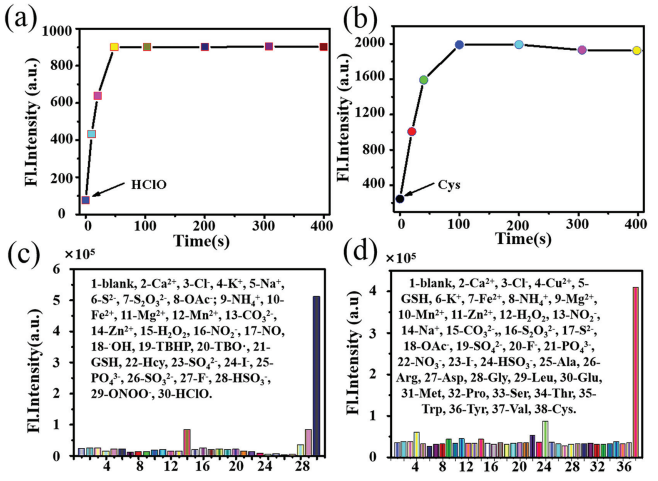

Fig. 3. Kinetics of probe **HP** response to HClO (a) and Cys (b). (c) Selectivity of probe **HP** (10 μmol/L) upon various species (2 mmol/L, HClO: 200 μmol/L). (d) Selectivity of probe **HP** (10 μmol/L) upon various species (20 mmol/L, Cys: 2 mmol/L). HClO: λ_{ex} = 660 nm, λ_{em} = 685 nm; Cys: λ_{ex} = 450 nm, λ_{em} = 495 nm. FI., fluorescence.

peak of methylene blue was not observed at first, but the absorption peak at 450 nm was gradually restored to that of the probe itself, and then by continuing to increase HClO, the absorption peak at 460 nm was basically unchanged, while the characteristic absorption peak of methylene blue was displayed. Similarly, the fluorescence spectra showed the same trend, after pre-treating the probe with 200 μmol/L Cys, the fluorescence intensity at 495 nm increased, and with the continued addition of HClO, we found that the fluorescence intensity at 495 nm decreased, and that the fluorescence intensity at 550 nm gradually recovered to that of the probe **HP** itself, and then, by continuing to add HClO, the fluorescence began to appear at 685 nm and was enhanced with the increase of HClO. These results confirmed that the probe **HP** could respond to HClO and Cys with different fluorescence signal patterns.

The development of highly selective probes was of great importance to investigate the role of bioactive molecules in pathogenesis and development. In parallel, we investigated the selectivity of probe **HP** for Cys and HClO (Fig. 3). Only HClO caused fluorescence enhancement at 685 nm, while other species including reactive oxygen species and reactive nitrogen species did not cause significant changes in the fluorescence spectra. Meanwhile, only Cys led to significant fluorescence enhancement at 495 nm. Of these, homocysteine (Hcy), which had similar properties to Cys, as well as glutathione (GSH), deserved special mention. In mammalian cells, the concentration of Hcy was in the range of 5–15 μmol/L, and the concentration of Cys was in the range of 30–200 μmol/L. When we added only 20 μmol/L Hcy to the probe solution, the absorption peak at 460 nm was basically unchanged. When 200 μmol/L Hcy was added to the probe solution until 13 min later, the absorption peak at 460 nm was slightly reduced and the fluorescence intensity at 550 nm was nearly negligible. When only 200 μmol/L Cys was added to the probe solution, the absorption peak at 460 nm was significantly reduced and blueshifted to 450 nm even after 5 min, and the fluorescence intensity at 550 nm blueshifted to 495 nm. If 200 μmol/L Cys and 200 μmol/L Hcy were added to the probe solution at the same time, it could be seen that 200 μmol/L Cys caused the absorption peak at 460 nm to decrease more distinctly and blueshifted, and in the fluorescence spectra, the fluorescence intensity at 550 nm was blueshifted to 495 nm with the increase of time and the fluorescence at 495 nm was gradually enhanced. In addition, the fluorescence intensity at 550 nm was essentially unchanged when 2 mmol/L or even 20 mmol/L GSH was added to the probe-containing system (Figs. S10, S11 and S13 in Supporting information). These results indicated that the probe had a high ability to selectively detect the target. Further, since the metabolism of reactive oxygen species as well as reactive sulphur and other substances *in vivo* was relatively rapid, rapid monitoring of their changes was also very important, and we evaluated the kinetic response of the probe to HClO and Cys, respectively, and found that a stable plateau was reached rapidly, which was quite advantageous for the monitoring of the probe *in vivo*. The physiological environment was a complex system, and the pH of its microenvironment varied from organelle to organelle. We therefore simulated various pH environments *in vitro* to assess the utility of the probe. As shown in Fig. S12 (Supporting information), the fluorescence intensity of probe **HP** hardly changed over a wide pH range. Upon addition of HClO, the fluorescence of probe **HP** at 685 nm was significantly enhanced at pH values between 4.0 and 10.0. Meanwhile, the mixture of probe **HP** and Cys showed strong fluorescence at 495 nm at pH values between 5.0 and 10.0. These results indicated that probe **HP** had good stability and it had high sensitivity and selectivity to Cys and HClO, suggesting that it had the potential to display both Cys and HClO by different fluorescence signals in biological systems.

Subsequently, we evaluated the probe's utility for biological visualization applications. First, we investigated the ability of the probe to image HClO and Cys within HeLa cells. As shown in Figs. 4a and b, after the probe was incubated with HeLa cells for 10 min, the green channel emitted weak fluorescence, and the red channel was almost no fluorescence. Considering the inherent Cys in the cells, we firstly used *N*-ethylmaleimide (NEM) to inhibit the production of Cys in the cells, and it could be observed that the fluorescence of the green channel disappeared, and the red channel was basically unchanged. Continuing with the pretreatment of HeLa cells with Cys for 0.5 h followed by incubation with probe **HP** for 10 min, then showed strong green fluorescence. When HeLa cells were pretreated with 200 μmol/L HClO and then incubated with 10 μmol/L probe **HP** for 10 min, the fluorescence of the red channel was switched on and the fluorescence intensity of the green channel was almost unchanged. We also examined the continuous imaging ability of the probe **HP** in live cells, and after suc-

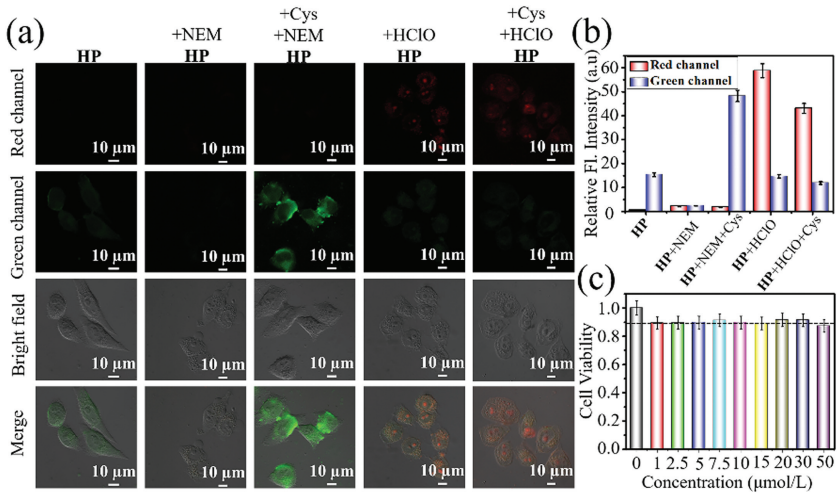

Fig. 4. (a) Individual and successive images of HClO and Cys in HeLa cells (NEM, 200 μmol/L, 0.5 h). (b) Fluorescence quantification corresponding to (a). (c) Cell viability values were estimated by CCK-8 assay for HeLa cells cultured in the presence of 0, 1, 2.5, 5, 7.5, 10, 15, 20, 30, and 50 μmol/L **HP** for 12 h. Red channel: λ_{em}= 655–715 nm (λ_{ex}= 633 nm); green channel: λ_{em}= 465–525 nm (λ_{ex}= 458 nm) Scale bar: 10 μm. The data were shown as mean ± standard deviation (SD) (n = 3).

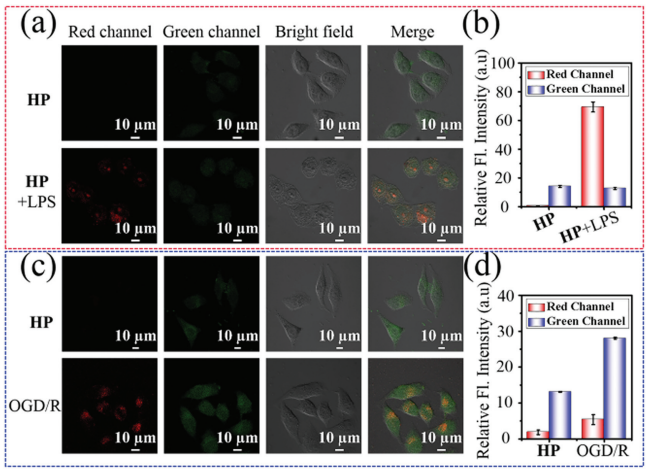

Fig. 5. Imaging of endogenous Cys or HClO in the HeLa cells with 10 μmol/L probe **HP**. (a) HeLa cells pre-treated with 1 μg/mL LPS for 0.5 h, then incubated with 10 μmol/L probe **HP**. (b) Fluorescence quantification corresponding to (a). OGD/R HeLa cells incubated with 10 μmol/L probe **HP**. (d) Fluorescence quantification corresponding to (c). Red channel: λ_{em}= 655–715 nm, λ_{ex}= 633 nm; green channel: λ_{em}= 465–525 nm, λ_{ex}= 458 nm. Scale bar: 10 μm. The data were shown as mean ± SD (n = 3).

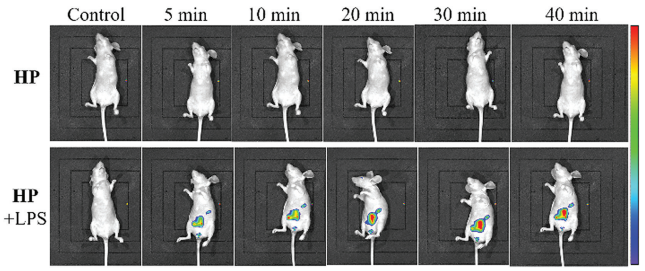

Fig. 6. Imaging of endogenous HClO in a mouse model of peritonitis. Mice were stimulated with LPS for 4 h and then injected with probe **HP**. Red channel: 710–750 nm; green channel: 500–520 nm.

cessive additions of HClO and Cys, significant fluorescent signals were detected in both channels. This demonstrated that probe **HP** could be used not only for individual imaging, but also for sequential imaging of HClO, Cys, and HClO/Cys in the red and green channels without interfering with each other. Further, we evaluated the biocompatibility of probe **HP** using cell counting kit-8 (CCK-8) toxicity assay. As shown in the Fig. 4c, the probe showed low cytotoxicity to cells. The above results showed that the probe had good biocompatibility and was of practical value for visual differentiation of bioactive molecules.

When the probe **HP** was incubated with HeLa cells for 10 min, the green channel emitted weak fluorescence and the red channel almost no fluorescence, indicating that the probe **HP** could detect endogenous Cys (Figs. 5a and b). There was evidence that cells produced endogenous HClO when stimulated with LPS. Unsurprisingly, when HeLa cells were treated with LPS, a significant fluorescent signal appeared in the red channel, whereas fluorescence in the green channel was essentially unchanged. Oxidative stress was an important cytopathological state that led to an imbalance in the cellular redox state. In order to study and evaluate the dynamics and correlation between HClO and Cys under oxidative stress, we utilized the OGD/R model. HeLa cells were cultured in sugar-free DMEM containing 0.5 mmol/L sodium bisulphite for 30 min, followed by another 30 min in high sugar DMEM. As shown in Fig. 5c, HeLa cells in the OGD/R group showed brighter green and red fluorescence compared to the control group. This suggested that under oxidative stress, the elevated reactive oxygen species HClO was accompanied by elevated Cys, which might be related to cellular self-regulation as a means of mitigating oxidative damage.

Studies had shown that inflammation was closely linked to oxidative stress and that endogenous production of excess HClO was a key mediator of inflammation. Based on the ability of probe **HP** to image HClO and Cys, we further applied probe **HP** to observe the dynamics of endogenous HClO and Cys in a mouse model of peritonitis. All the animal experiments were performed by following the protocols approved by the Radiation Protection Institute of Drug Safety Evaluation Center in China (Production license: SYXK (Jin) 2018–0005). All animal experiments were performed according to the protocols approved by the Animal Ethics and Use Committee. Mice model of peritonitis was established by intraperitoneal injection of LPS (2 mg/mL, 100 μL) into female BALB/c mice for 4 h (Fig. 6). Subsequently, mice were injected with 200 mmol/L (200 μL) of probe **HP**. As shown in the Fig. 6, fluorescence was observed in the abdomen of the mice immediately after 5 min of injection, while no fluorescence was observed in the abdomen of the control group, and then the signals of the experimental group reached the maximum value at about 30 min. The results of the

above experiments suggested that the probe **HP** could be used to assess changes in HClO levels in a mouse model of peritonitis. As an effective fluorescent probe, probe **HP** could be used to diagnose peritonitis by monitoring fluctuations in HClO levels.

In summary, the importance and challenge of monitoring redox homeostasis dynamics in complex living systems enabled us to design and develop a dual response fluorescent probe **HP** based on the binding of methylene blue and coumarin for the individual and continuous detection of HClO and Cys. The probe rapidly produced different fluorescence signals for HClO and Cys with good sensitivity and excellent selectivity. It was worth mentioning that this probe has good specificity for Cys. In addition, we successfully demonstrated that the probe **HP** was a useful tool for monitoring HClO- and Cys-mediated redox homeostasis in living cells as well as fluctuations in HClO levels in mouse peritonitis. Overall, this study provides a platform to analyze and visualize two opposing biologically active species that can inform the design of other chemical sensors aimed at gaining insight into redox homeostasis.

Declaration of competing interest

The authors declare that they have no known competing financial interests or personal relationships that could have appeared to influence the work reported in this paper.

Acknowledgments

We thank the National Natural Science Foundation of China (Nos. 22207069, 22325703, 22377071, 22074084), Research Project Supported by Shanxi Scholarship Council of China (No. 2022-002), the Shanxi Province Science Foundation (Nos. 20210302124012, 202203021221009), Key R&D and transformation plan of Qinghai Province (No. 2020-GX-101), 2023 Graduate Innovation Project of Shanxi University.

Supplementary materials

Supplementary material associated with this article can be found, in the online version, at doi:10.1016/j.cclet.2024.109778.

References

[1] H. Sies, C. Berndt, D.P. Jones, Annu. Rev. Biochem. 86 (2017) 715–748.
[2] J. Nguyen, A. Tirla, P. Rivera-Fuentes, Org. Biomol. Chem. 19 (2021) 2681–2687.
[3] N. Yang, R.R. Zheng, Z.Y. Chen, et al., Biomater. Sci. 10 (2022) 1575–1581.
[4] E. Zebrowska, A. Chabowski, A. Zalewska, M. Maciejczyk, Nutrients 12 (2020) 3181.
[5] H.Q. Ju, Y.X. Lu, Q.N. Wu, et al., Oncogene 36 (2017) 6282–6292.
[6] X.F. Yang, Y. Zheng, L.Y. Zheng, J. Photochem. Photobiol. A 424 (2022) 113575.
[7] P. Jia, Z.H. Zhuang, C.Y. Liu, et al., Anal. Chim. Acta 1052 (2019) 131–136.
[8] T. Henrique de Araujo, S.S. Okada, E.E.B. Ghosn, et al., Cell. Immunol. 281 (2013) 27–30.
[9] Y.M. Yang, Q. Zhao, W. Feng, F.Y. Li, Chem. Rev. 113 (2013) 192–270.
[10] L. Roland, M. Ulrich, Annu. Rev. Cell Dev. Biol. 22 (2006) 457–486.
[11] W. Eranthie, C. Wang, M.S. Gabriel, et al., Nature 468 (2010) 790–795.
[12] J.K. Andersen, Nat. Med. 10 (2004) S18–S25.
[13] M. Whiteman, N.S. Cheung, Y.Z. Zhu, et al., Biochem. Biophys. Res. Commun. 326 (2005) 794–798.
[14] Z.Q. Mao, M.T. Ye, W. Hu, et al., Chem. Sci. 9 (2018) 6035–6040.
[15] K.J. Wang, D.Z. Xi, C.T. Liu, et al., Chin. Chem. Lett. 31 (2020) 2955–2959.
[16] S.J. Li, K. Yang, Y. Liu, et al., Sens. Actuators B: Chem. 379 (2023) 133253.
[17] M. Chen, X.Y. Chen, Y. Wang, et al., Sens. Actuators B: Chem. 371 (2022) 132545.
[18] X.B. Wang, H.J. Li, Q.H. Li, et al., J. Hazard. Mater. 427 (2022) 127874.
[19] Y. Yuan, S.Z. Xiong, L.Q. Lv, et al., Chem. Eng. J. 471 (2023) 144341.
[20] R. Li, W.X. Li, R. Chen, W.Y. Lin, Sens. Actuators B: Chem. 347 (2021) 130616.
[21] J.C. Qin, Z.W. Li, Z.H. Fu, Z.H. Zhang, Sens. Actuators B: Chem. 357 (2022) 131430.
[22] X.K. Yang, J.M. Wang, Z.L. Zhang, et al., Food Biochem. 416 (2023) 135730.
[23] R. Chen, W.X. Li, R. Li, et al., Chin. Chem. Lett. 34 (2023) 107845.
[24] D. Liu, X.X. Yue, H.K. Zhang, et al., Dyes Pigm. 215 (2023) 111257.
[25] S.J. Li, P.P. Wang, K. Yang, et al., Anal. Chim. Acta 1252 (2023) 341009.
[26] Y.M. Shen, J.L. Jin, Y.D. Chen, Y.C. Tang, Microchem. J. 195 (2023) 109424.
[27] W.X. Qiu, Z.Y. Xu, Z. Sun, N.B. Li, H.Q. Luo, Sens. Actuators B: Chem. 394 (2023) 134357.
[28] G.W. Fan, B. Zhang, J.M. Wang, et al., Talanta 268 (2024) 125298.
[29] C.L. Liu, Z.P. Li, H. Zhang, et al., Anal. Chim. Acta 1279 (2023) 341779.
[30] G.Q. Fu, Q. Song, Z.Q. Wang, et al., Anal. Chem. 95 (2023) 17559–17567.
[31] B. Wu, T.H. Xue, Y.N. He, et al., Chin. Chem. Lett. 32 (2021) 932–937.
[32] Q.S. Gu, Z.C. Yang, J.J. Chao, et al., Anal. Chem. 95 (2023) 12478–12486.
[33] Y.K. Zhang, C. Xu, H. Sun, M.G. Ren, F.G. Kong, J. Photochem. Photobiol. A 444 (2023) 114919.
[34] S.S. Long, Q. Luo, B.B. Yuan, et al., Dyes Pigm. 220 (2023) 111688.
[35] L.F. Wang, J. Liu, M.H. Ren, W. Guo, Chin. Chem. Lett. 35 (2024) 108945.
[36] R. He, D.D. Tang, N.G. Xu, et al., Chin. Chem. Lett. 35 (2024) 108658.
[37] S.X. An, Y.F. Lin, T.Q. Ye, et al., Talanta 267 (2024) 125247.
[38] B.X. Zhang, H.J. Zhang, M. Zhong, et al., Chin. Chem. Lett. 31 (2020) 133–135.
[39] H.J. Wang, W.W. Xing, Z.H. Yu, et al., Chin. Chem. Lett. 35 (2024) 109183.
[40] X.D. Ding, B. Yang, Z.L. Liu, et al., Anal. Chim. Acta 1280 (2023) 341873.
[41] Y.D. Cheng, X. Wang, J. Chen, et al., Chin. Chem. Lett. 35 (2024) 109156.
[42] C. Cao, J. Zhou, X.L. Zhang, et al., Spectrochim. Acta Part A 305 (2024) 123429.
[43] W.Y. Liao, S.W. Zhang, X.W. Wang, et al., Dyes Pigm. 219 (2023) 111649.